



Gas hydrates exist as crystalline structures, and water molecules enclose smaller gas molecules such as methane (Sloan et al., 2008). Natural gas hydrates are stored in permafrost sediments and offshore sea beds because gas hydrates are stable in low temperature and high pressure conditions (Sloan, 2003). Natural gas hydrates, mostly methane hydrates, are considered an unconventional energy source because of the large amount of deposits on the Earth (Mikov, 2004). Gas hydrate production projects are ongoing world-widely, mainly in the US, Canada and Japan.

The stable condition of natural gas hydrates is determined by the pressure and temperature conditions seen in the phase diagram of Fig. 1. The depressurization method reduces the pressure below the stable pressure of the gas hydrates causing the hydrates to dissociate into water and methane gas. The pressure reduction is caused by pore water pumping through the production well in which dissociated methane gas and water are produced. During the pumping, the hydraulic conductivity of gas hydrate-bearing sediments has an important role in the productivity and dissociation rate. Gas hydrates obstruct the flow of liquid and gas phase materials because gas hydrates fill the voids between soil particles. Therefore, gas hydrate saturation has an effect on the water and gas permeability.

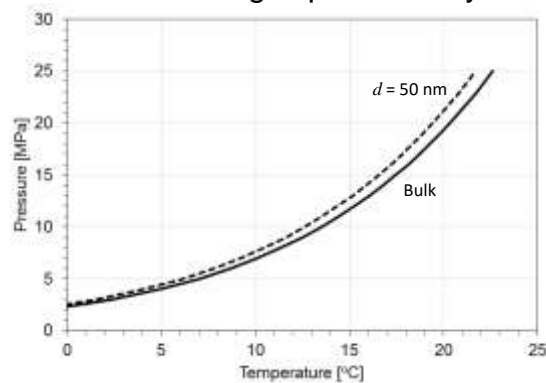


Fig. 1 CO<sub>2</sub> gas hydrate stability diagram

High gas hydrate saturation (over 60%) reduces water permeability almost 100 times lower than zero gas hydrate saturation (Mohana, 2014). Therefore, the relation between gas hydrate saturation and hydraulic conductivity is important for the productivity and dissociation rate during gas hydrate production.

## 2. EXPERIMENTAL PROGRAM

### 2.1 Specimen

During deep drilling expeditions in 2007 and 2010, 13 drill sites were explored. Among the drilled sites, UBGH2-6 was chosen as one of the potential production test sites taking into consideration the presence of gas hydrates and the composition of the sediment layers. A comparison of the grain size distribution between the artificial specimen and the core sample from UBGH2-6 is shown in Fig. 2. The specimen is silty sand with a specific gravity of 2.62 and mean particle size of 130  $\mu\text{m}$ .

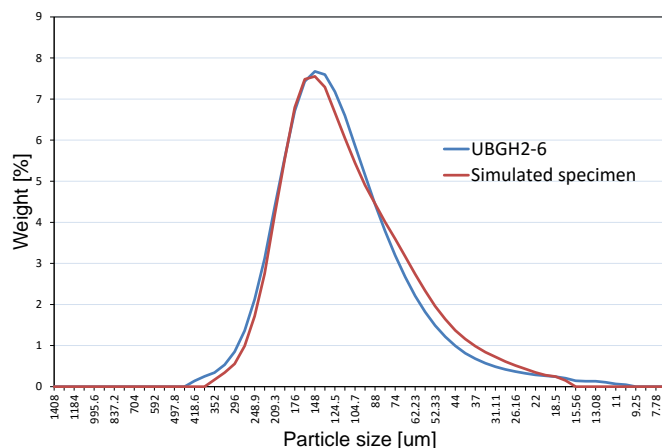


Fig. 2 Grain size distribution

### 2.2 Experimental setup

Fig. 3 shows a schematic diagram of the experiment apparatus for gas hydrate formation and permeability measurements. CO<sub>2</sub> gas was injected from the top of the specimen, and water was injected from both sides of the specimen. P- and S-wave velocities and electrical resistance were measured at the lateral side of the specimen with a signal generator and oscilloscope. Two syringe pumps were located at the upper and lower sides of the specimen to control the pressure.

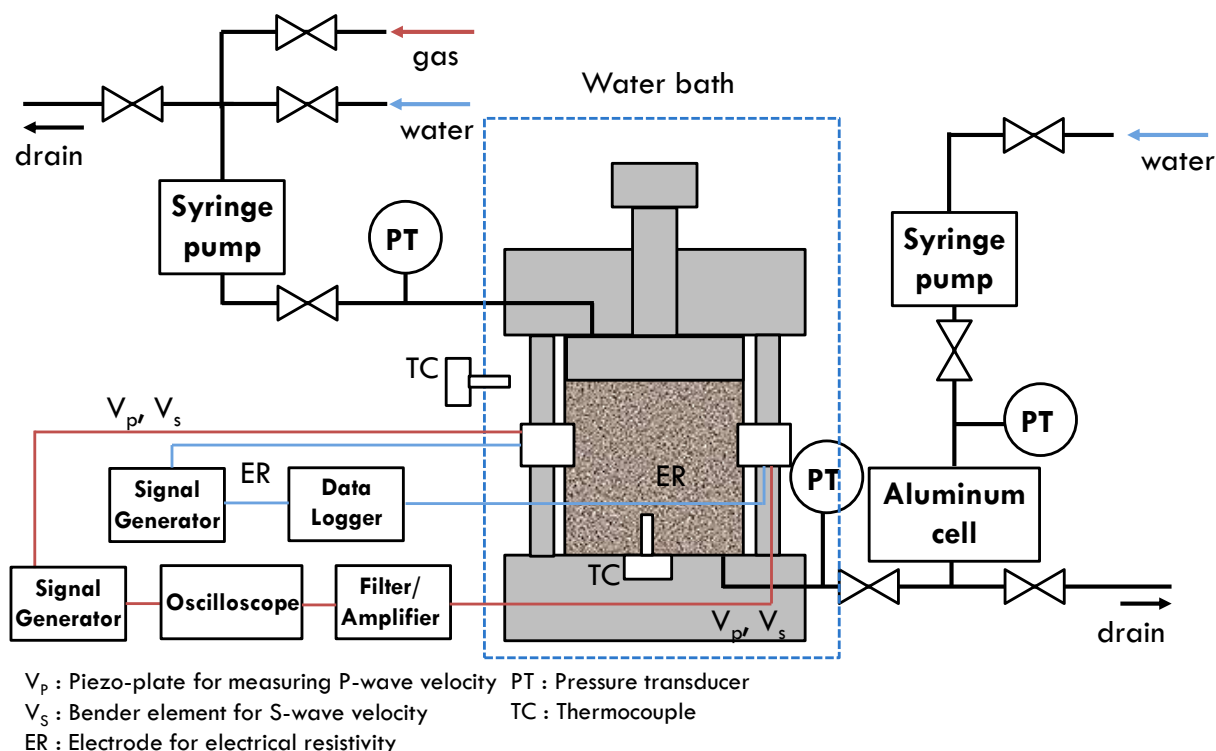


Fig. 3 Experimental setup

### 2.3 Experimental procedure

The initial gas hydrate saturation is determined by the partial water saturation of the specimen. CO<sub>2</sub> gas injection and system cooling are carried out using the appropriate pressure and temperature for CO<sub>2</sub> gas hydrate formation. After the formation of gas hydrates in the specimen, water is injected until fully saturated.

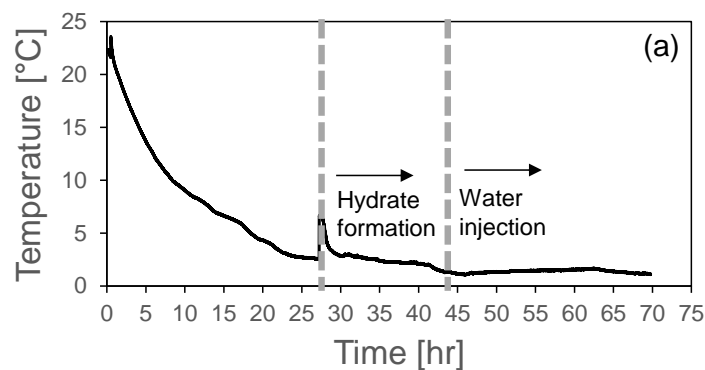
The permeability measurement is controlled by the syringe pumps at the upper and lower sides of the specimen. In order to saturate specimen with water, injection pressure was 2.8 MPa. The permeability measurement was conducted for several hours with a 50 kPa difference because low permeability in gas hydrate-bearing sediments is expected.

Gas hydrate saturation is calculated by capturing CO<sub>2</sub> gas during the dissociation of the gas hydrates. Gas hydrate dissociation is performed by step-wise depressurization. During the gas hydrate dissociation and capturing of CO<sub>2</sub> gas, the measured volume of the CO<sub>2</sub> gas represents the decrease in the gas hydrate saturation of the specimen. Gas hydrate dissociation and capturing of CO<sub>2</sub> gas continue until dissociation is completion. The temperature, pressure and wave velocities are measured during the entire experiment to monitor gas hydrate saturation.

### 3. EXPERIMENTAL RESULTS

#### 3.1 Gas hydrate formation

The initial porosity was 0.58, and the void ratio was 1.39. From the calculation, the initial gas hydrate saturation was 0.49. Gas hydrate formation and water saturation were monitored by the temperature and P- and S-wave velocities shown in Fig. 4.



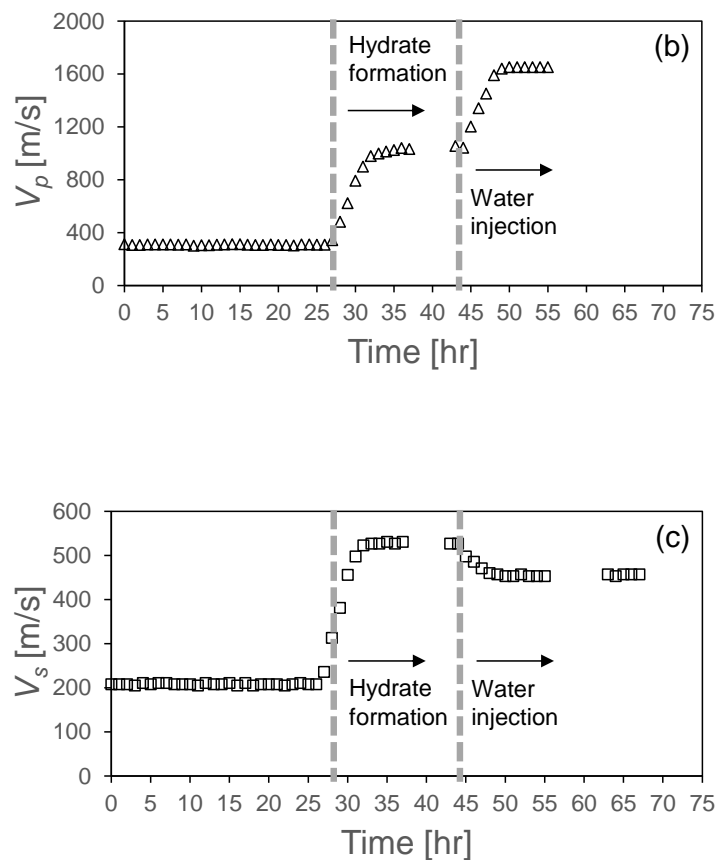


Fig. 4 (a) Temperature (b) P-wave velocity (c) S-wave velocity change with time

As shown in Fig. 4(a), a sudden temperature enhancement of about 4°C occurs during gas hydrate formation. The exothermic reaction of gas hydrate formation increases the temperature of the specimen instantly. The stiffening effect of the gas hydrates result in a wave velocity increase in Fig. 4(b) and Fig. 4(c). After water injection, the P-wave velocity is increased because of the compressional wave characteristics of the P-wave. Otherwise, the S-wave velocity decreases after water injection. The S-wave velocity is only affected by the soil skeleton which implies a decrease in gas hydrate saturation. A partial pressure difference between the injected water and gas hydrates causes the dissociation of gas hydrates as pure water is injected.

### 3.2 Permeability

The experimental result for water permeability with gas hydrate saturation is shown in Fig. 5. Measurement of the permeability was done at a gas hydrate saturation of 37%, 22% and 0%. Water permeability at a gas hydrate saturation of 37% was about 2.1 times lower than that at 22% gas hydrate saturation. Otherwise, the water permeability without any gas hydrates present was almost  $10^2$  times bigger than result for the 37% gas hydrate saturation. This large difference implies that the existence of

gas hydrates obstructs fluid flow along the pores. Permeability coefficient was about  $10^{-9}$  m/s in gas hydrate-bearing sediments in the Ulleung basin of Korea.

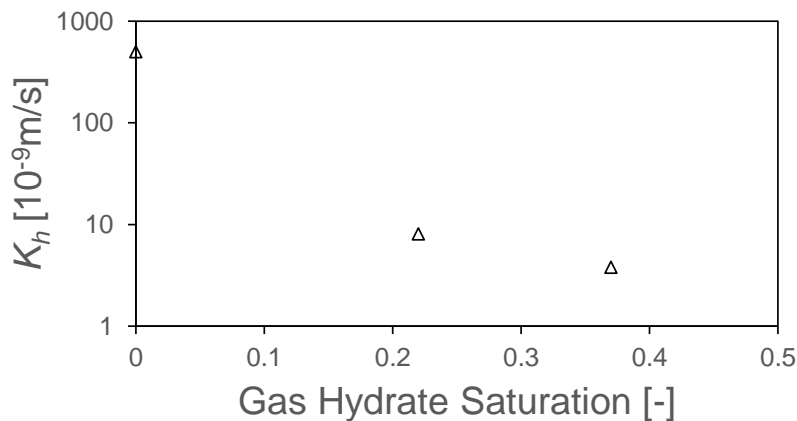


Fig. 5 Water permeability with gas hydrate saturation

#### 4. CONCLUSIONS

Water permeability measurements were performed with 0%, 22% and 37% gas hydrate saturation within an artificial specimen of the core sample from gas hydrate-bearing sediments. The permeability of the gas hydrate-bearing specimen was  $10^2$  times lower than the specimen without gas hydrates. This result shows the remarkable effect of gas hydrate saturation on the permeability of sediments. Precise empirical model for permeability with gas hydrate saturation can be established by additional permeability experiments with various gas hydrate saturation condition.

#### ACKNOWLEDGEMENT

This research was supported by the Basic Research Project of the Korea Institute of Geoscience and Mineral Resources (KIGAM) funded by the Ministry of Knowledge Economy of Korea and the "U-City Master and Doctor Course Grant (Education) Program" under the Korea Ministry of Land, Infrastructure and Transport (MOLIT).

#### REFERENCES

- Milkov, A. V. (2004), "Global estimates of hydrate-bound gas in marine sediments: how much is really out there?", *Earth Science Reviews*, **66**(3), 183-197.
- Mohana, L. D. and Jocelyn L. H. Grozic (2014), "Experimental determination of permeability of porous media in presence of gas hydrates", *J. of Petroleum Science and Engineering*, **120**, 1-9.

*The 2016 World Congress on  
Advances in Civil, Environmental, and Materials Research (ACEM16)  
Jeju Island, Korea, August 28-September 1, 2016*

- Sloan, E. D. and Koh, C. A. (2008), "Clathrate Hydrates of Natural Gases 3<sup>rd</sup> ed.", CRC Press, Boca Raton, Florida.
- Sloan, E. D. (2003), "Fundamental principles and applications of natural gas hydrates", *Nature*, **426**, 353-363.
- Zhao, J., Zhu, Z., Song, Y., Liu, W., Zhang, Y. and Wang, D. (2014), "Analyzing the process of gas production for natural gas hydrate using depressurization", *Applied Energy*, **142**, 125-134.